

Precision Mass Measurements of Neutron-Rich Scandium Isotopes Refine the Evolution of $N = 32$ and $N = 34$ Shell Closures

E. Leistenschneider^{1,2,*} E. Dunling^{3,4} G. Bollen,^{1,2,5} B. A. Brown,^{1,2,5} J. Dilling,^{3,6} A. Hamaker^{1,2,5}
 J. D. Holt,^{3,7} A. Jacobs,^{3,6} A. A. Kwiatkowski,^{3,8} T. Miyagi³ W. S. Porter^{3,6} D. Puentes^{1,2,5} M. Redshaw^{9,2}
 M. P. Reiter^{3,10,11} R. Ringle^{1,2} R. Sandler,⁹ C. S. Sumithrarachchi,^{1,2} A. A. Valverde,¹² and I. T. Yandow^{1,2,5}

The LEBIT Collaboration and the TITAN Collaboration

¹Facility for Rare Isotope Beams, Michigan State University, East Lansing, Michigan 48824, USA

²National Superconducting Cyclotron Laboratory, Michigan State University, East Lansing, Michigan 48824, USA

³TRIUMF, 4004 Wesbrook Mall, Vancouver, British Columbia V6T 2A3, Canada

⁴Department of Physics, University of York, York YO10 5DD, United Kingdom

⁵Department of Physics and Astronomy, Michigan State University, East Lansing, Michigan 48824, USA

⁶Department of Physics & Astronomy, University of British Columbia, Vancouver, British Columbia V6T 1Z1, Canada

⁷Department of Physics, McGill University, 3600 Rue University, Montréal, Québec H3A 2T8, Canada

⁸Department of Physics and Astronomy, University of Victoria, Victoria, British Columbia V8P 5C2, Canada

⁹Department of Physics, Central Michigan University, Mount Pleasant, Michigan 48859, USA

¹⁰II. Physikalisches Institut, Justus-Liebig-Universität, 35392 Gießen, Germany

¹¹School of Physics and Astronomy, University of Edinburgh, Edinburgh EH9 3FD, United Kingdom

¹²Department of Physics & Astronomy, University of Manitoba, Winnipeg, Manitoba R3T 2N2, Canada



(Received 1 June 2020; revised 28 September 2020; accepted 14 December 2020; published 26 January 2021)

We report high-precision mass measurements of $^{50-55}\text{Sc}$ isotopes performed at the LEBIT facility at NSCL and at the TITAN facility at TRIUMF. Our results provide a substantial reduction of their uncertainties and indicate significant deviations, up to 0.7 MeV, from the previously recommended mass values for $^{53-55}\text{Sc}$. The results of this work provide an important update to the description of emerging closed-shell phenomena at neutron numbers $N = 32$ and $N = 34$ above proton-magic $Z = 20$. In particular, they finally enable a complete and precise characterization of the trends in ground state binding energies along the $N = 32$ isotone, confirming that the empirical neutron shell gap energies peak at the doubly magic ^{52}Ca . Moreover, our data, combined with other recent measurements, do not support the existence of a closed neutron shell in ^{55}Sc at $N = 34$. The results were compared to predictions from both *ab initio* and phenomenological nuclear theories, which all had success describing $N = 32$ neutron shell gap energies but were highly disparate in the description of the $N = 34$ isotone.

DOI: [10.1103/PhysRevLett.126.042501](https://doi.org/10.1103/PhysRevLett.126.042501)

The formation of simple, periodic patterns is a key to understanding the organization of countless many-body systems [1]. In the case of atomic nuclei, clear repetition of special properties, such as enhanced binding energy, are seen in “magic” proton and neutron numbers (like 2, 8, 20, 28, 50, ...), which led to the proposition that nucleons organize themselves into shell-like structures, analogous to atomic electron orbitals. Today, the nuclear shell model [2] constitutes the foundation of our understanding of these objects. However, once believed to be immutable, these magic nucleon numbers are now known to vanish and new ones to appear in extreme cases of proton-to-neutron ratio [3]. The appearance and evolution of emerging shell closures have become standard metrics to benchmark nuclear theories [4,5].

Emerging closed shell phenomena have been observed for neutron-rich nuclei at neutron numbers $N = 32$ and $N = 34$ at and around the proton-magic calcium chain ($Z = 20$). Such behaviors at $N = 32$ were found through several observables. Mass spectrometry experiments identified peaks in empirical neutron shell gap energies in ^{51}K ($Z = 19$) [6], ^{52}Ca ($Z = 20$) [5,7], ^{53}Sc ($Z = 21$) [8], and ^{54}Ti ($Z = 22$) [9], but not in ^{55}V ($Z = 23$) [10] and higher proton numbers. This shell closure is also seen in enhanced 2^+ excitation energies at ^{50}Ar ($Z = 18$) [11], ^{52}Ca [12], ^{54}Ti [13], and ^{56}Cr ($Z = 24$) [14], and reduced $B(E2)$ transition probabilities in ^{54}Ti [15] and ^{56}Cr [16]. In $N = 34$, albeit less experimentally studied, evidence of a shell closure was observed in the mass of ^{54}Ca [17] and in the 2^+ excitation energies of ^{54}Ca [18,19] and ^{52}Ar [20].

In the shell model, a magic number appears when there is a significant energy gap between two nucleon orbitals. In $N = 32$ nuclei with more than 24 protons, neutrons in the valence $p_{3/2}$ orbital are quasidegenerate with those in the next orbital— $f_{5/2}$ —thus no appreciable energy gap is observed. As protons are removed, a strong residual interaction between protons and neutrons weakens, causing a migration of the neutron $f_{5/2}$ energy level, a widened gap with the $p_{3/2}$, and thus the formation of the $N = 32$ shell closure [4]. Subsequently, as the proton number drops below $Z = 23$ and the proton-neutron residual interaction further wanes, an energy level inversion between the neutron orbitals $f_{5/2}$ and $p_{1/2}$ occurs [13,18]. The next neutron orbital— $p_{1/2}$ —then has a degeneracy of 2, allowing also for the formation of the $N = 34$ shell closure provided that a significant gap can be formed with the $f_{5/2}$ orbital.

The conjoint structural changes at $N = 32$ and 34 provide a unique opportunity to refine our understanding of nuclear interactions and the intricate nuclear many-body problem [4,5,9]. Therefore, detailed information on how the characteristic observables evolve with increments in proton number is of paramount importance. Above $Z = 20$, the evolution of the $N = 32$ shell closure is nearly resolved, but a few outstanding issues remain. Among them, recent Isochronous Mass Spectrometry (IMS) measurements suggest the empirical neutron shell gap at $N = 32$ is unexpectedly higher in ^{53}Sc than in the doubly magic ^{52}Ca [8,21]. In $N = 34$, experimental evidence indicates an absence of closed shell signatures in Ti [13,22] and their presence in Ca [17–19] but, in between, the picture in Sc remains unclear [23–25].

These questions demand refined mass measurements of neutron-rich scandium isotopes, which remains the only chain in the region still unexplored using high-resolution techniques. In this Letter, we report precision mass measurements of $^{50-55}\text{Sc}$, between $N = 29$ and 34, performed in a joint collaboration between experimental groups at the National Superconducting Cyclotron Laboratory (NSCL) in the U.S. and at the TRIUMF National Laboratory in Canada.

At NSCL, the neutron-rich isotopes $^{50-53}\text{Sc}$ were produced in flight by nuclear fragmentation of a 130 MeV/u ^{76}Ge primary ion beam impinging on a natural Be target of about 0.4 g/cm² thickness. The beam was purified at the A1900 fragment separator [26] and delivered to the NSCL’s gas catcher [27], where the high-energy fragments were stopped in a high-purity He gas. The ions were extracted at low energies from the gas cell and selected in mass-to-charge ratio (A/Q) by a dipole magnet. The species of interest were extracted as singly charged molecules, mostly oxides, formed during stopping in the gas cell. The ion beam was then delivered to the Low Energy Beam and Ion Trap (LEBIT) facility [28].

LEBIT is an ion trap facility dedicated to performing high-precision mass spectrometry of short-lived ions [28].

The beam was received into LEBIT’s cooler and buncher [29], where the continuous rare isotope beam was converted into short low-emittance bunches. The ion bunches were then sent to LEBIT’s 9.4 T Penning trap mass spectrometer [30], where they were further purified against isobaric contaminants by applying a dipolar radio-frequency (RF) field [31,32].

The measurement of the mass (m_{ion}) of the ion is done through the measurement of the frequency (ν_c) of the cyclotron motion about the trap’s magnetic field: $\nu_c = (qB)/(2\pi m_{\text{ion}})$, where q is the charge of the ion and B is the strength of the magnetic field. To measure ν_c , we employed the time-of-flight ion-cyclotron-resonance (TOF-ICR) technique [33], using standard quadrupole excitation schemes ranging between 50 ms and 500 ms, depending on the measurement. Figure 1(a) shows a typical TOF-ICR spectrum obtained for $^{53}\text{Sc}^{16}\text{O}^+$.

The calibration of B was done through the measurement of the cyclotron frequency of a reference ion ($\nu_{c,\text{ref}}$), whose mass has been precisely measured and is well documented in the literature [34]. The reference ions were all well-known molecular ions produced in the gas catcher and delivered with the ion of interest, with the same A/Q . Measurements of $\nu_{c,\text{ref}}$ were performed at intervals not longer than 1.5 h, interleaved between measurements of ν_c of ions of interest, to account for temporal variations in the magnetic field.

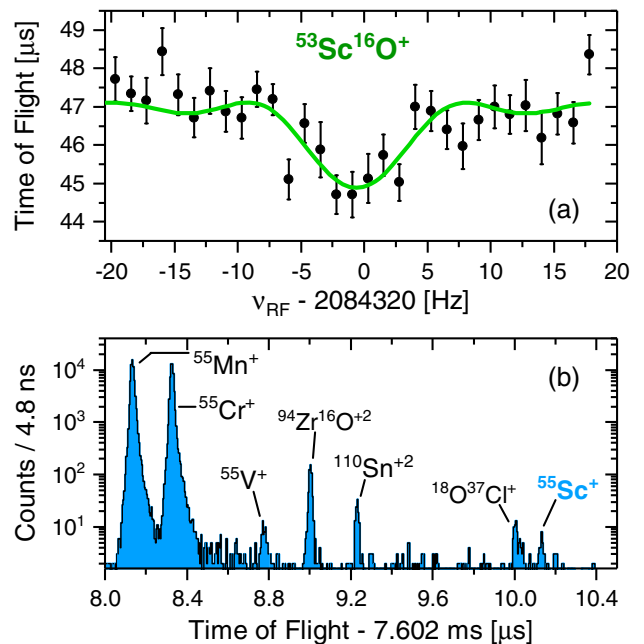


FIG. 1. A sample mass spectrum from each experiment: (a) A TOF-ICR spectrum of a $^{53}\text{Sc}^{16}\text{O}^+$ molecular ion, obtained with excitation time of 100 ms at LEBIT. The dip in time of flight occurs at ν_c , extracted using an analytical fit (green). (b) A typical MR-TOF-MS spectrum at $A/Q = 55$ obtained at TITAN with 520 isochronous turns.

Each TOF-ICR spectrum was fitted with an analytical function described in Ref. [33], from which the cyclotron frequency was obtained. A count-rate class analysis [35] was performed to account for frequency shifts due to ion-ion interactions. The atomic mass of the species of interest (m) was determined from the ratio of cyclotron frequencies (R) of the ion of interest and the reference ion: $R = \nu_{c,\text{ref}}/\nu_c = (m - m_e)/(m_{\text{ref}} - m_e)$, where m_e is the mass of the electron and m_{ref} is the mass of the reference species (obtained from Ref. [34], summing the masses of all atoms of the molecule). This equation is valid for singly ionized species and it disregards insignificant electron and molecular binding energies, on the order of a few eV or less. $\nu_{c,\text{ref}}$ was obtained from an interpolation, to the time of the measurement of the ion of interest, between the reference measurements before and after it. The mass of the nuclide of interest is obtained by subtracting the masses of its molecular counterparts.

At TRIUMF, samples of ^{54}Sc and ^{55}Sc were produced via the isotope separation on-line (ISOL) method through spallation reactions at the Isotope Separator and ACcelerator (ISAC) [36] facility by impinging a 480 MeV proton beam of $50 \mu\text{A}$ onto a Ta target, 22.7 g/cm^2 thick. The reaction products were stopped and thermalized in the target material, released through desorption, and surface ionized at the TRILIS ion source [37]. The beam was extracted from the target, selected in A/Q at ISAC's dipole mass separator [38] and delivered at low energy to TRIUMF's Ion Trap for Atomic and Nuclear science (TITAN) facility [39].

The radioactive beam was accumulated at TITAN's cooler and buncher [40] for 20 ms and sent as ion bunches to the Multiple-Reflection Time-of-Flight Mass Spectrometer (MR-TOF-MS) [41]. The MR-TOF-MS determines the mass of a charged particle through its time-of-flight through a standardized path at known kinetic energy [42,43]. In order to increase the measurement resolution, this device confines the ion by bouncing it between a pair of electrostatic mirrors, recycling and thus extending the flight path and preserving the initial time spread. In this experiment, the bunches were received by the MR-TOF-MS in an internal ion preparation system

composed by gas-filled RF quadrupoles [41], where ions were recooled for about 13 ms. The ions were then sent to the mass analyzer for times of flight of about 7.5 ms, where they underwent 520 isochronous turns between the mirrors. Finally, they were detected by a MagneTOF detector [44]. An in-analyzer mass-range selector, similar to Ref. [45], was used to remove any particle outside the desired A/Q window. Also, to prevent ion-ion interaction effects, the average count rate was kept below 2 counts/cycle.

A typical time of flight spectrum is shown in Fig. 1(b). Every peak in the MR-TOF-MS spectra was fitted using a Gaussian function. The spectra were mass calibrated using the nonrelativistic relationship: $m_{\text{ion}}/q = C(t_{\text{tof}} - t_0)^2$, where C and t_0 are calibration constants and t_{tof} is the fitted centroid of the peak. The parameter t_0 is a constant delay caused in the signal processing and was determined using off-line measurements. In both spectra taken with $A/Q = 54$ and 55 , we identified the presence of isobaric singly charged Cr, Fe, Mn, V, Ti, Sc, and several molecules. Stable $^{54,55}\text{Cr}^+$ formed dominant peaks in their spectra and, therefore, were chosen as suitable calibrants for C using their atomic mass values available in the literature [34]. A time-dependent calibration, similar to Ref. [46], was used to account for drifts in time of flight. A mass resolving power of about 200000 was achieved, and a total of 236 counts of ^{54}Sc and 35 counts of ^{55}Sc were registered.

The atomic masses of the species of interest were determined through the relationship $m = m_{\text{ion}} + m_e$, which disregards electron binding energies. A relative systematic uncertainty of 3×10^{-7} was added following the prescription outlined in previous experiments [9,10,47], as well as an additional relative uncertainty of 1.9×10^{-7} to account for ion-ion interaction effects [48].

The masses obtained in both experiments are reported in Table I with comparisons with the recommended values by the Atomic Mass Evaluation of 2016 (AME16) [34]. The precision was improved in all cases, some by over an order of magnitude, to the scale of a few tens of keV or better. Deviations were found, up to 0.7 MeV, in the masses of $^{53-55}\text{Sc}$ ($N = 32-34$), which can significantly impact the description of nuclear structure phenomena.

TABLE I. Results of the mass measurements performed, compared to the values recommended by the AME16 [34]. We also provide the mass ratio between the ion of interest and the reference ion, which is equivalent to the average cyclotron frequency ratio (R) for the LEBIT TOF-ICR data. All mass values are in keV.

Facility	Nuclide	Mass excess	Literature [34]	Difference	Ion of interest	Reference ion	Mass ratio
LEBIT	^{50}Sc	-44537.1 (2.5)	-44547(15)	10 (15)	$^{50}\text{Sc}^{16}\text{O}^+$	$^{12}\text{C}^{19}\text{F}^{35}\text{Cl}^+$	0.999 694 485 (41)
	^{51}Sc	-43250.4 (2.5)	-43229(20)	-22(20)	$^{51}\text{Sc}^{16}\text{O}^+\text{H}^+$	$^{33}\text{S}^{19}\text{F}^{16}\text{O}^+$	0.999 875 402 (39)
	^{52}Sc	-40523.6 (3.0)	-40443(82)	-80(82)	$^{52}\text{Sc}^{16}\text{O}^+$	$^{33}\text{S}^{19}\text{F}^{16}\text{O}^+$	0.999 803 339 (48)
	^{53}Sc	-38769(17)	-38907(94)	138 (96)	$^{53}\text{Sc}^{16}\text{O}^+$	$^{34}\text{S}^{19}\text{F}^{16}\text{O}^+$	0.999 885 58 (27)
TITAN	^{54}Sc	-34438(18)	-33891(270)	-547(270)	$^{54}\text{Sc}^+$	$^{54}\text{Cr}^+$	1.000 447 76 (36)
	^{55}Sc	-30842(62)	-30159(450)	-683(460)	$^{55}\text{Sc}^+$	$^{55}\text{Cr}^+$	1.000 474 2 (12)

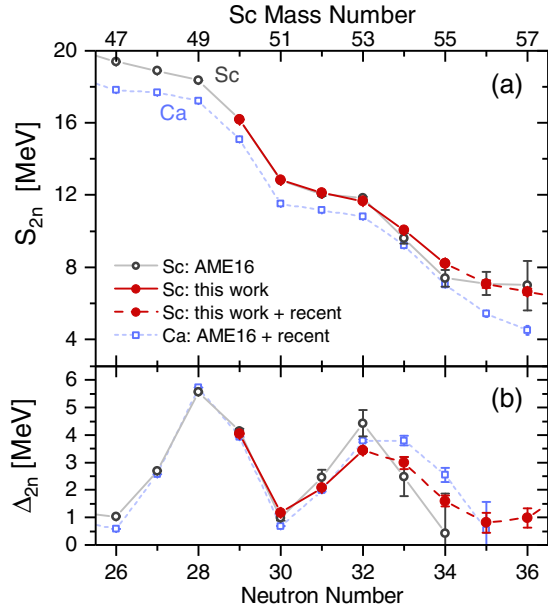


FIG. 2. Derivatives of the mass surface around neutron numbers $N = 28, 32, 34$: (a) S_{2n} and (b) Δ_{2n} of Sc isotopes as a function of N . Our results (red circles) provide a 2σ lower Δ_{2n} at $N = 32$ compared to the AME16 [34] (gray). Results from Refs. [25,49] were used to compound our Δ_{2n} at $N \geq 33$ (dashed). The proton-magic calcium chain (blue squares) was added for reference, with data from Refs. [17,34].

Because of the strong binding character of closed shells, nucleons added on top of them are appreciably less bound. Hence, closed neutron shells can be identified by sudden decreases in two-neutron separation energies, defined as $S_{2n}(Z, N) = [m(Z, N - 2) + 2m_n - m(Z, N)]c^2$, where m_n is the mass of the neutron. These changes in slopes are emphasized by looking at derivatives of S_{2n} , known as empirical shell gaps: $\Delta_{2n}(Z, N) = S_{2n}(Z, N) - S_{2n}(Z, N + 2)$. Figure 2 shows S_{2n} and Δ_{2n} for scandium isotopes employing our values and AME16 values [34]. Consecutive sharp features are clearly seen at $N = 28$, a “canonical” magic number, and at $N = 32$, an “emerging” magic number. Our results confirm a strong $N = 32$ sub-shell closure in ^{53}Sc , but provide a 1 MeV lower (2σ away) empirical neutron shell gap energy (3.45 ± 0.06 MeV) than the AME16 and the most recent experimental result [8] (4.4 ± 0.5 MeV).

Our update to the empirical neutron shell gap of ^{53}Sc considerably impacts the evolution of the $N = 32$ shell closure and finally permits its inspection using only high-resolution mass data. Figure 3 shows Δ_{2n} as a function of Z for isotones of interest in the region, combining mass values from AME16 [34], recent experiments [8–10,17,25], and our data. Clearly, the shell gap at $N = 32$ evolves smoothly without abrupt changes, mirroring the evolution of the canonical $N = 28$ shell but ≈ 2 MeV lower. With our data, Δ_{2n} increases monotonically through ^{53}Sc and peaks at ^{52}Ca , consistent with the latter being a doubly magic nucleus.

To derive Δ_{2n} towards $N = 34$, we incorporated mass values of $^{56,57}\text{Sc}$ from two recent Time-of-flight Magnetic Rigidity experiments at NSCL [25] and RIKEN [49]. The trends in S_{2n} in Sc seem to indicate the restoration of nonclosed shell slope after $N = 34$. It contrasts with the Ca chain, where the continuation of a sharp slope through $N = 34$ is evidence of the existence of a shell closure [17]. We update the Δ_{2n} at ^{55}Sc to 1.59 ± 0.20 MeV. This is the lowest empirical neutron shell gap in the $N = 34$ isotone, as can be seen in Fig. 3. High-resolution mass measurements of $^{56,57}\text{Sc}$ are required to confirm the observed trends.

As our data enable a more consistent picture of the evolution of both $N = 32$ and 34 isotones, we compared Δ_{2n} data with predictions from state-of-the-art nuclear models, which are included in Fig. 3. We chose four approaches that had great success in describing closed shell features at $N = 32$. Among phenomenological approaches, we performed shell model calculations using the KB3G [50] and the GX1A [51] Hamiltonians for all nuclei from Ca ($Z = 20$) to Fe ($Z = 26$) between $N = 26$ and $N = 36$, using the full pf model space. Both interactions have been successful in predicting trends in binding energies [5,7,17,25], excitation energies [15,52,53], and transition strengths [15,16] associated with emerging closed shells in the region. Among *ab initio* approaches, we employed valence-space in-medium similarity renormalization group [54,55] (VS-IMSRG) calculations with the 1.8/2.0(EM) [56] and the NN + 3N(Inl) [57] interactions. The 1.8/2.0(EM) interaction has been extensively employed in the region and adequately predicted the presence of the $N = 32$ closed shell in the mass surface [8,9,56,58,59]. This approach has also had success in describing excitation energies around this isotone [20,24,56], and trends of charge radii in neutron-rich Ca isotopes [60]. The NN + 3N(Inl) interaction, released more recently, has also correctly predicted closed shell behaviors in the region [9,19,57,61] and has shown a comparable performance to the 1.8/2.0(EM) interaction. Our work is the first application of the NN + 3N(Inl) interaction within the VS-IMSRG approach, which also enables the analysis of its performance across different many-body methods.

Overall, the trends up to $N = 32$ are well reproduced by all predictions. In particular, the KB3G interaction produces excellent agreement with data, not only reproducing trends but also magnitudes of shell gaps along most of the $N = 28, 32$ isotones. Also, both VS-IMSRG calculations correctly reproduce the observed trends, although they overpredict the strength of shell gaps at $N = 32$ [9,56]. The calculations with the NN + 3N(Inl) interaction have poorer performance at $N = 28, 30$ but produce nearly identical results as the 1.8/2.0(EM) interaction in the region of the emerging shell closures. The GX1A interaction, however, produces a less pronounced evolution of the $N = 32$ isotone, peaking at ^{54}Ti and not at the double-magic ^{52}Ca .

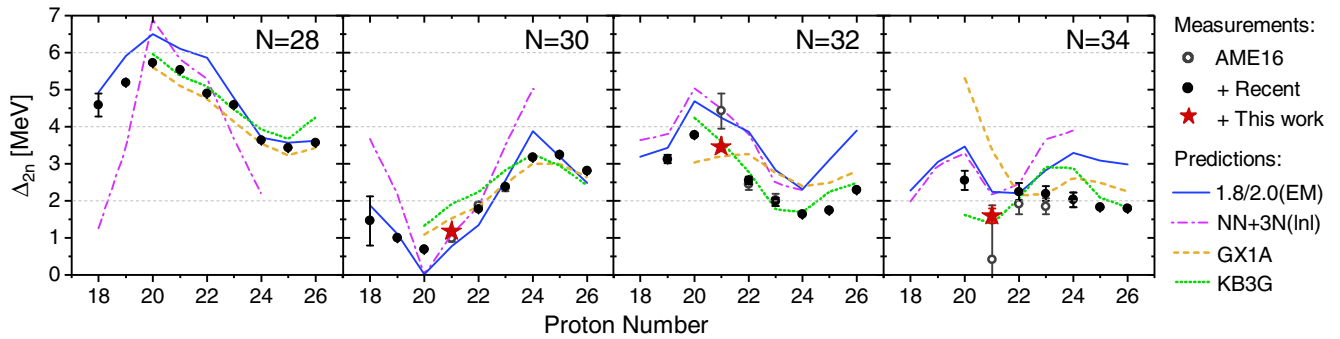


FIG. 3. Measured (points) and predicted (lines) empirical neutron shell gaps for isotones in the region of interest: the canonical magic $N = 28$, the nonmagic $N = 30$, the emerging magic $N = 32$, and the possibly magic $N = 34$. Measured points include the AME16 [34] (open circles), with recent measurements [9,10,17,49] (full circles), and our work (with Refs. [25,49]) (red stars). Predictions include VS-IMSRG calculations using 1.8/2.0(EM) (solid blue line) and $NN + 3N(\text{Inl})$ (pink dash-dotted line) chiral Hamiltonians, and shell model calculations using KB3G (green dotted line) and GX1A (yellow dashed line) phenomenological Hamiltonians.

The theoretical predictions are highly disparate regarding the description of the $N = 34$ shell gap. The GX1A interaction predicts a strong shell gap at ^{54}Ca , which is not observed. The KB3G reproduces well Δ_{2n} in ^{55}Sc and ^{56}Ti , but does not predict the emergence of closed shell behaviors at ^{54}Ca . A similar discrepancy has also been observed in descriptions of 2^+ excitation energy using these interactions [18,52,53]. The 2^+ state of ^{54}Ca lies 2.04(2) MeV above the ground state [18]. According to our calculations with the GX1A interaction, it lies at 2.96 MeV, while KB3G predicts 1.34 MeV. Both VS-IMSRG calculations are in better agreement with $N = 34$ data at $Z \leq 22$. Most remarkably, they reproduce the Δ_{2n} leap between ^{55}Sc and ^{54}Ca , but predict Δ_{2n} to reduce towards argon ($Z = 18$). It conflicts with recent γ -spectrometry results, that indicate $N = 34$ closed shell behaviors overcomes $N = 32$ in strength at Ar [11,20].

In summary, we performed high-precision mass measurements of $^{50-53}\text{Sc}$ at the LEBIT facility at NSCL and of $^{54,55}\text{Sc}$ at the TITAN facility at TRIUMF. With our mass values, we obtained a smooth and monotonic evolution of the $N = 32$ neutron shell gaps above $Z = 20$, finally completing the mass description of the emergence of this closed shell using high-resolution methods. The observed behavior conforms to typical shell evolution as confirmed by various theoretical predictions, both from phenomenological and *ab initio* approaches. Our results support ^{52}Ca as a doubly magic nucleus, establishing it as the peak of empirical shell gaps instead of ^{53}Sc . Regarding the possibly emerging closed shell at $N = 34$, our results combined with recent data from [25,49] suggest that closed-shell behaviors only appear in the mass surface at $Z \leq 20$. Our analysis also explored some theoretical approaches that have had superior performance in describing emerging closed shell behaviors in the region. Despite the proposed intimate relationship between the emergence of closed shells in $N = 32$ and 34, success in describing observables in $N = 32$ is not correlated with similar successes in $N = 34$.

The authors would like to thank J. Simonis and P. Navrátil for providing the 1.8/2.0(EM) and $NN + 3N(\text{Inl})$ matrix element files and S.R. Stroberg for the IMSRG++ code [62] used to perform the VS-IMSRG calculations. We are grateful to Z. Meisel for the fruitful discussions regarding data obtained in previous experiments. We also thank NSCL staff, the ISAC Beam Delivery group, the TRILIS group, and M. Good for their technical support, as well as J. Bergmann for his assistance with analysis software employed in this work. This work was conducted with the support of Michigan State University, the U.S. National Science Foundation under Contracts No. PHY-1565546 and No. PHY-1811855, the U.S. Department of Energy, Office of Science, Office of Nuclear Physics under Award No. DE-SC0015927, the Natural Sciences and Engineering Research Council (NSERC) of Canada through Contract No. SAPPJ-2018-00015 and the National Research Council (NRC) of Canada through TRIUMF. E. D. acknowledges financial support from the U.K.-Canada foundation. M. P. R. acknowledges support from BMBF (Grants No. 05P16RGFN1 and No. 05P19RGFN8), Hessisches Ministerium für Wissenschaft und Kunst (HMWK) through the LOEWE Center HICforFAIR, by the JLU and GSI Helmholtzzentrum für Schwerionenforschung under the JLU-GSI strategic Helmholtz partnership agreement. A. A. V. acknowledges support from NSERC (Canada) under Contract No. SAPPJ-2018-00028.

*Corresponding author.
leistenschneider@frib.msu.edu

- [1] R. F. G. Ruiz and A. R. Vernon, Emergence of simple patterns in many-body systems: From macroscopic objects to the atomic nucleus, *Eur. Phys. J. A* **56**, 136 (2020).
- [2] M. Mayer and J. Jensen, *Elementary Theory of Nuclear Shell Structure*, Structure of Matter Series (John Wiley & Sons, New York, 1955).

- [3] D. Warner, Nuclear physics: Not-so-magic numbers, *Nature (London)* **430**, 517 (2004).
- [4] T. Otsuka, A. Gade, O. Sorlin, T. Suzuki, and Y. Utsuno, Evolution of shell structure in exotic nuclei, *Rev. Mod. Phys.* **92**, 015002 (2020).
- [5] F. Wienholtz *et al.*, Masses of exotic calcium isotopes pin down nuclear forces, *Nature (London)* **498**, 346 (2013).
- [6] M. Rosenbusch *et al.*, Probing the $N = 32$ Shell Closure below the Magic Proton Number $Z = 20$: Mass Measurements of the Exotic Isotopes $^{52,53}\text{K}$, *Phys. Rev. Lett.* **114**, 202501 (2015).
- [7] A. T. Gallant *et al.*, New Precision Mass Measurements of Neutron-Rich Calcium and Potassium Isotopes and Three-Nucleon Forces, *Phys. Rev. Lett.* **109**, 032506 (2012).
- [8] X. Xu *et al.*, Masses of neutron-rich $^{52-54}\text{Sc}$ and $^{54,56}\text{Ti}$ nuclides: The $N = 32$ subshell closure in scandium, *Phys. Rev. C* **99**, 064303 (2019).
- [9] E. Leistenschneider *et al.*, Dawning of the $N = 32$ Shell Closure Seen through Precision Mass Measurements of Neutron-Rich Titanium Isotopes, *Phys. Rev. Lett.* **120**, 062503 (2018).
- [10] M. P. Reiter *et al.*, Quenching of the $N = 32$ neutron shell closure studied via precision mass measurements of neutron-rich vanadium isotopes, *Phys. Rev. C* **98**, 024310 (2018).
- [11] D. Steppenbeck *et al.*, Low-Lying Structure of ^{50}Ar and the $N = 32$ Subshell Closure, *Phys. Rev. Lett.* **114**, 252501 (2015).
- [12] A. Huck, G. Klotz, A. Knipper, C. Miehé, C. Richard-Serre, G. Walter, A. Poves, H. L. Ravn, and G. Marguier, Beta decay of the new isotopes ^{52}K , ^{52}Ca , and ^{52}Sc ; a test of the shell model far from stability, *Phys. Rev. C* **31**, 2226 (1985).
- [13] S. N. Liddick *et al.*, Development of shell closures at $N = 32, 34$. I. β decay of neutron-rich Sc isotopes, *Phys. Rev. C* **70**, 064303 (2004).
- [14] J. Prisciandaro, P. Mantica, B. Brown, D. Anthony, M. Cooper, A. Garcia, D. Groh, A. Komives, W. Kumarasiri, P. Lofy, A. Oros-Peusquens, S. Tabor, and M. Wiedeking, New evidence for a subshell gap at $N = 32$, *Phys. Lett. B* **510**, 17 (2001).
- [15] A. Goldkuhle *et al.* (AGATA Collaboration), Lifetime measurements in $^{52,54}\text{Ti}$ to study shell evolution toward $N = 32$, *Phys. Rev. C* **100**, 054317 (2019).
- [16] M. Seidlitz *et al.*, Precision lifetime measurements of the first 2^+ and 4^+ states in ^{56}Cr at the $N = 32$ subshell closure, *Phys. Rev. C* **84**, 034318 (2011).
- [17] S. Michimasa *et al.*, Magic Nature of Neutrons in ^{54}Ca : First Mass Measurements of $^{55-57}\text{Ca}$, *Phys. Rev. Lett.* **121**, 022506 (2018).
- [18] D. Steppenbeck *et al.*, Evidence for a new nuclear ‘magic number’ from the level structure of ^{54}Ca , *Nature (London)* **502**, 207 (2013).
- [19] S. Chen *et al.*, Quasifree Neutron Knockout from ^{54}Ca Corroborates Arising $N = 34$ Neutron Magic Number, *Phys. Rev. Lett.* **123**, 142501 (2019).
- [20] H. N. Liu *et al.*, How Robust is the $N = 34$ Subshell Closure? First Spectroscopy of ^{52}Ar , *Phys. Rev. Lett.* **122**, 072502 (2019).
- [21] X. Xu *et al.*, Direct mass measurements of neutron-rich ^{86}Kr projectile fragments and the persistence of neutron magic number $N = 32$ in Sc isotopes, *Chin. Phys. C* **39**, 104001 (2015).
- [22] D.-C. Dinca *et al.*, Reduced transition probabilities to the first 2^+ state in $^{52,54,56}\text{Ti}$ and development of shell closures at $N = 32, 34$, *Phys. Rev. C* **71**, 041302(R) (2005).
- [23] H. L. Crawford, R. V. F. Janssens, P. F. Mantica, J. S. Berryman, R. Broda, M. P. Carpenter, N. Cieplicka, B. Fornal, G. F. Grinyer, N. Hoteling, B. P. Kay, T. Lauritsen, K. Minamisono, I. Stefanescu, J. B. Stoker, W. B. Walters, and S. Zhu, β decay and isomeric properties of neutron-rich Ca and Sc isotopes, *Phys. Rev. C* **82**, 014311 (2010).
- [24] D. Steppenbeck *et al.*, Structure of ^{55}Sc and development of the $N = 34$ subshell closure, *Phys. Rev. C* **96**, 064310 (2017).
- [25] Z. Meisel *et al.*, Nuclear mass measurements map the structure of atomic nuclei and accreting neutron stars, *Phys. Rev. C* **101**, 052801(R) (2020).
- [26] D. Morrissey, B. Sherrill, M. Steiner, A. Stolz, and I. Wiedenhoever, Commissioning the A1900 projectile fragment separator, *Nucl. Instrum. Methods Phys. Res., Sect. B* **204**, 90 (2003).
- [27] C. Sumithrarachchi, D. Morrissey, S. Schwarz, K. Lund, G. Bollen, R. Ringle, G. Savard, and A. Villari, Beam thermalization in a large gas catcher, *Nucl. Instrum. Methods Phys. Res., Sect. B* **463**, 305 (2020).
- [28] R. Ringle, S. Schwarz, and G. Bollen, Penning trap mass spectrometry of rare isotopes produced via projectile fragmentation at the LEBIT facility, *Int. J. Mass Spectrom.* **349–350**, 87 (2013), 100 years of Mass Spectrometry.
- [29] S. Schwarz, G. Bollen, R. Ringle, J. Savory, and P. Schury, The LEBIT ion cooler and buncher, *Nucl. Instrum. Methods Phys. Res., Sect. A* **816**, 131 (2016).
- [30] R. Ringle, G. Bollen, A. Prinke, J. Savory, P. Schury, S. Schwarz, and T. Sun, The LEBIT 9.4 T Penning trap mass spectrometer, *Nucl. Instrum. Methods Phys. Res., Sect. A* **604**, 536 (2009).
- [31] M. Kretzschmar, Theoretical investigations of different excitation modes for Penning trap mass spectrometry, *Int. J. Mass Spectrom.* **349–350**, 227 (2013).
- [32] A. Kwiatkowski, G. Bollen, M. Redshaw, R. Ringle, and S. Schwarz, Isobaric beam purification for high precision Penning trap mass spectrometry of radioactive isotope beams with SWIFT, *Int. J. Mass Spectrom.* **379**, 9 (2015).
- [33] M. König, G. Bollen, H.-J. Kluge, T. Otto, and J. Szerypo, Quadrupole excitation of stored ion motion at the true cyclotron frequency, *Int. J. Mass Spectrom. Ion Process.* **142**, 95 (1995).
- [34] W. Huang, G. Audi, M. Wang, F. G. Kondev, S. Naimi, and X. Xu, The AME2016 atomic mass evaluation (I). Evaluation of input data; and adjustment procedures, *Chin. Phys. C* **41**, 030002 (2017);
- [35] A. Kellerbauer, K. Blaum, G. Bollen, F. Herfurth, H.-J. Kluge, M. Kuckein, E. Sauvan, C. Scheidenberger, and L. Schweikhard, From direct to absolute mass measurements: A study of the accuracy of ISOLTRAP, *Eur. Phys. J. D* **22**, 53 (2003).
- [36] G. C. Ball, G. Hackman, and R. Krücken, The TRIUMF-ISAC facility: Two decades of discovery with rare isotope beams, *Phys. Scr.* **91**, 093002 (2016).

- [37] J. Lassen, P. Bricault, M. Dombbsky, J. P. Lavoie, M. Gillner, T. Gottwald, F. Hellbusch, A. Teigelhöfer, A. Voss, and K. D. A. Wendt, Laser ion source operation at the TRIUMF radioactive ion beam facility, *AIP Conf. Proc.* **1104**, 9 (2009).
- [38] P. Bricault, R. Baartman, M. Dombbsky, A. Hurst, C. Mark, G. Stanford, and P. Schmor, TRIUMF-ISAC target station and mass separator commissioning, *Nucl. Phys.* **A701**, 49 (2002).
- [39] J. Dilling, R. Baartman, P. Bricault, M. Brodeur, L. Blomeley, F. Buchinger, J. Crawford, J. R. C. López-Urrutia, P. Delheij, M. Froese, G. P. Gwinner, Z. Ke, J. K. P. Lee, R. B. Moore, V. Ryjov, G. Sikler, M. Smith, J. Ullrich, and J. Vaz, Mass measurements on highly charged radioactive ions, a new approach to high precision with TITAN, *Int. J. Mass Spectrom.* **251**, 198 (2006).
- [40] T. Brunner, M. J. Smith, M. Brodeur, S. Ettenauer, A. T. Gallant, V. V. Simon, A. Chaudhuri, A. Lapierre, E. Mané, R. Ringle, M. C. Simon, J. A. Vaz, P. Delheij, M. Good, M. R. Pearson, and J. Dilling, TITAN's digital RFQ ion beam cooler and buncher, operation and performance, *Nucl. Instrum. Methods Phys. Res., Sect. A* **676**, 32 (2012).
- [41] C. Jesch, T. Dickel, W. R. Plaß, D. Short, S. Ayet San Andres, J. Dilling, H. Geissel, F. Greiner, J. Lang, K. G. Leach, W. Lippert, C. Scheidenberger, and M. I. Yavor, The MR-TOF-MS isobar separator for the TITAN facility at TRIUMF, *Hyperfine Interact.* **235**, 97 (2015).
- [42] H. Wollnik and M. Przewloka, Time-of-flight mass spectrometers with multiply reflected ion trajectories, *Int. J. Mass Spectrom. Ion Process.* **96**, 267 (1990).
- [43] W. R. Plaß, T. Dickel, and C. Scheidenberger, Multiple-reflection time-of-flight mass spectrometry, *Int. J. Mass Spectrom.* **349**, 134 (2013).
- [44] T. Dickel, S. A. San Andrés, S. Beck, J. Bergmann, J. Dilling, F. Greiner, C. Hornung, A. Jacobs, G. Kripko-Koncz, A. Kwiatkowski, E. Leistenschneider, A. Pikhtelev, W. R. Plaß, M. P. Reiter, C. Scheidenberger, C. Will, and for the TITAN Collaboration, Recent upgrades of the multiple-reflection time-of-flight mass spectrometer at TITAN, TRIUMF, *Hyperfine Interact.* **240**, 62 (2019).
- [45] T. Dickel, W. R. Plaß, A. Becker, U. Czok, H. Geissel, E. Haettner, C. Jesch, W. Kinsel, M. Petrick, C. Scheidenberger, A. Simon, and M. I. Yavor, A high-performance multiple-reflection time-of-flight mass spectrometer and isobar separator for the research with exotic nuclei, *Nucl. Instrum. Methods Phys. Res., Sect. A* **777**, 172 (2015).
- [46] S. Ayet San Andrés *et al.*, High-resolution, accurate multiple-reflection time-of-flight mass spectrometry for short-lived, exotic nuclei of a few events in their ground and low-lying isomeric states, *Phys. Rev. C* **99**, 064313 (2019).
- [47] M. P. Reiter *et al.*, Mass measurements of neutron-rich gallium isotopes refine production of nuclei of the first r -process abundance peak in neutron-star merger calculations, *Phys. Rev. C* **101**, 025803 (2020).
- [48] E. Dunling *et al.*, Towards new frontiers: Systematic investigation of uncertainties of the TITAN multiple-reflection time-of-flight mass spectrometer and isobar separator (to be published).
- [49] S. Michimasa *et al.*, Mapping of a New Deformation Region around ^{62}Ti , *Phys. Rev. Lett.* **125**, 122501 (2020).
- [50] A. Poves, J. Snchez-Solano, E. Caurier, and F. Nowacki, Shell model study of the isobaric chains $A = 50$, $A = 51$ and $A = 52$, *Nucl. Phys.* **A694**, 157 (2001).
- [51] M. Honma, T. Otsuka, B. A. Brown, and T. Mizusaki, New effective interaction for pf -shell nuclei and its implications for the stability of the $N = Z = 28$ closed core, *Phys. Rev. C* **69**, 034335 (2004).
- [52] J. D. Holt, T. Otsuka, A. Schwenk, and T. Suzuki, Three-body forces and shell structure in calcium isotopes, *J. Phys. G* **39**, 085111 (2012).
- [53] M. Honma, T. Otsuka, B. A. Brown, and T. Mizusaki, Shell-model description of neutron-rich pf -shell nuclei with a new effective interaction GXPf-1, *Eur. Phys. J. A* **25**, 499 (2005).
- [54] S. R. Stroberg, H. Hergert, J. D. Holt, S. K. Bogner, and A. Schwenk, Ground and excited states of doubly open-shell nuclei from ab initio valence-space Hamiltonians, *Phys. Rev. C* **93**, 051301(R) (2016).
- [55] S. R. Stroberg, A. Calci, H. Hergert, J. D. Holt, S. K. Bogner, R. Roth, and A. Schwenk, Nucleus-Dependent Valence-Space Approach to Nuclear Structure, *Phys. Rev. Lett.* **118**, 032502 (2017).
- [56] J. Simonis, S. R. Stroberg, K. Hebeler, J. D. Holt, and A. Schwenk, Saturation with chiral interactions and consequences for finite nuclei, *Phys. Rev. C* **96**, 014303 (2017).
- [57] V. Somà, P. Navrátil, F. Raimondi, C. Barbieri, and T. Duguet, Novel chiral hamiltonian and observables in light and medium-mass nuclei, *Phys. Rev. C* **101**, 014318 (2020).
- [58] M. Mougeot *et al.*, Precision Mass Measurements of $^{58-63}\text{Cr}$: Nuclear Collectivity Towards the $N = 40$ Island of Inversion, *Phys. Rev. Lett.* **120**, 232501 (2018).
- [59] S. R. Stroberg, J. D. Holt, A. Schwenk, and J. Simonis, *Ab initio* limits of atomic nuclei, *Phys. Rev. Lett.* **126**, 022501 (2021).
- [60] R. F. Garcia Ruiz *et al.*, Unexpectedly large charge radii of neutron-rich calcium isotopes, *Nat. Phys.* **12**, 594 (2016).
- [61] V. Somà, C. Barbieri, T. Duguet, and P. Navrátil, Moving away from singly-magic nuclei with Gorkov Green's function theory, [arXiv:2009.01829](https://arxiv.org/abs/2009.01829).
- [62] S. R. Stroberg, In-medium similarity renormalization group software for nuclear structure calculations, <https://github.com/ragnarstroberg/imsrg>.